Start-up of Modular Three-stage SST

Mariam Saeed, José María Cuartas*, Alberto Rodríguez, Manuel Arias and Fernando Briz
University of Oviedo, Department of Electrical Engineering
*INAEL Electrical Systems, Toledo, Spain

***Abstract* -- This paper discusses the start-up of modular three-stage Solid State Transformers (SSTs) based on a cascaded H-bridge (CHB) topology. Auxiliary Power Supplies (APSs) are used to feed the auxiliary circuitry from the cells DC link. Since DC links need to charge to a certain threshold voltage to power the APSs, then first steps of the start-up must be performed before APSs are operative and consequently without measurements and control. This can result in undesirable events, e.g. inrush currents, voltage sags in the capacitors voltages, etc. In this work a start-up scheme for the SST is proposed. The procedure is valid for both grid-forming and grid-feeding SST operation modes. Simulation and experimental results are provided.**

***Index Terms*—Solid state Transformers, start-up, auxiliary power supplies.**

I. Introduction

Solid State Transformers (SSTs), also called Power Electronic Transformers or Smart Transformers, are a power electronics-based alternative to Line Frequency Transformer (LFTs). SSTs are based on power semiconductors, sensors and controls. This enable them to provide advanced functionalities, including: power flow control; reactive power, harmonics and imbalances compensation; smart protection and ride-through capabilities. In addition, the high switching frequencies of the semiconductors enable a significant reduction of the volume and weight of the core material used in their isolation stages [1]-[4]. Examples of applications in which SSTs can be advantageous are: smart-grid applications that require an efficient integration of distributed generation and storage resources, flexible routing mechanisms, active filtering and protection mechanism. Traction, off-shore and subsea systems are space-critical applications in which the improved performances and power density of SSTs compared to LFTs can be relevant [5], [6].

There are two key aspects in the design of an SST: number of stages and modularity. According to the number of stages, SSTs with one, two and three stages have been reported [4]–[7]. Three-stage configurations allows optimization of each converter stage independently. In addition, it enormously simplifies control and commutation strategies, thanks to the storage elements (capacitors) in the connections. Reduction of the number of stages implies the use of matrix-type topologies, which complicates the design of control and protections. On the other hand, the use of modular multilevel SST topologies provides several advantages. Terminal voltages of the SST can be arbitrarily increased by serializing more cells. Redundancy and consequently fault tolerant designs are possible by adding spare cells. Modular designs produce multilevel voltage wave shapes, allowing a reduction of the switching frequency (and consequently of the switching losses) [8], facilitating the design of the output filter, etc.

While there is an extensive literature on the design, modeling, control, fault tolerance, etc. of SSTs, [9]-[13], very few works have discussed their energization and start-up. This includes 1) start-up of APSs feeding all elements used for control (digital controllers, sensors, drivers, etc.); 2) connection of the SST to the grids/loads through the corresponding pre-charge circuits, switchgears, etc. and 3) enabling the control-loops for normal operation of the SST. Furthermore, most of the work published on this topic deals with non-modular (even if they are multilevel) topologies. Charging the medium voltage (22 kV) DC link from the LV side in a 3L-NPC is discussed in [14]. In [15], the SST is a three-stage topology composed of a rectifier, a dual half-bridge (DHB) and an inverter. The authors proposed a straightforward stage-by-stage start-up scheme, and analyzed the problems related to the inrush current in the high-frequency transformer. In [16] a scheme aiming at minimizing the transformer current during the start-up by synchronizing rectifier and DC/DC converter stages is proposed. Strategies for the APSs design and start-up procedure in a modular three-stage SST is discussed in [17]. However, the work is focused on the validation of the APSs but no simulation or experimental results are provided.

Start-up of modular multilevel SSTs is especially challenging [18] because in these topologies stacked cells can be several kV over the global reference. APSs are used to supply the auxiliary electronics (controls, sensors, drivers, etc.) in each cell. Selection of the primary voltage source for the APSs is not trivial due to the high voltage levels and isolation requirements intrinsic to the modular design of the SST. It is advantageous to use APSs fed from the cell DC-link capacitors [19]. However, until the cell capacitors reach the minimum operating voltage level of the APS, the cell circuitry is not powered and consequently, there is no control of the power devices.

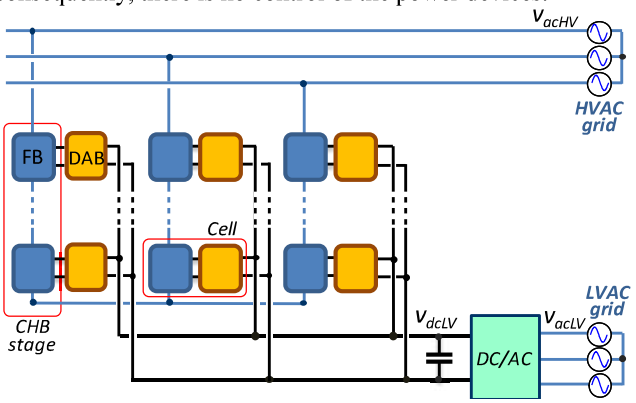

Fig. 1: Modular CHB based SST topology. LVAC and HVAC grid filters are not shown for the sake of simplicity.

Consequently, start-up of the APS and connection of the SST to the grid occurs simultaneously. The scenario is even worse if the voltage in one port must be established by the SST. Energization of this (secondary) port must be performed from the other (primary) port through the isolation transformers. However, this before all electronics of the secondary port are operative. This can lead to uncontrolled events during start-up such as inrush current, voltage sags in the capacitor voltages, etc.

This paper studies the start-up process for a three-stage modular SST based on a cascaded H-bridge (CHB). Start-up occurs in several steps but can be generally classified into two processes: 1) powering up the three converter stages by means of pre-stablished transients and 2) full SST closed loop control. The presented ideas are validated by simulation and experimental results. The paper is organized as follows: Section II discusses the selected SST topology and the modes of operation. Cells and SST start-up are addressed in Section III. Experimental results at the cell level are provided in Section IV. As the final SST prototype is not operative yet, Section V verifies the start-up of the SST using the proposed method by means of simulation. Finally, conclusions are presented in Section VI.

I. SST Modes of Operation

The selected SST topology is shown in Fig. 1. It uses a three-stage configuration [20], [21]. Its main characteristics are shown in Table I. The high-voltage (HV) side front-end AC/DC stage uses a Cascaded H-bridge structure. The intermediate stage uses Dual Active Bridge (DAB) DC/DC converters which provides the required isolation between HV and low-voltage (LV) AC ports. The outputs of all DABs are connected in parallel to provide a LV, high-current DC link, which is connected to the LV side DC/AC converter. HV side and isolating stages of the SST are seen to be fully modular, i.e. formed by identical stacked cells/modules. All the stages in Fig. 1 are controllable. Consequently, both HV and LV ports can operate either in a grid-feeding or in a grid-forming mode and with a bidirectional power flow. Grid-feeding is possible if the voltage in both ports is established externally by existing HV and LV AC grids. In grid-forming mode, the voltage in one port is established by the SST [20].

For proper operation of the SST, the grid must exist in at least one port, three potential working modes being possible:

1) Grid-forming in the HV (Fig. 2a). Voltage in the LV port is supplied externally. CHB stage establishes the voltage in the HV port. LV side DC/AC converter controls V_{dcLV}. DABs regulate cell voltages V_{cell}, while CHB stage controls HV side output voltage V_{acHV}.
2) Grid-forming in the LV side (Fig. 2b). Voltage in the HV port is supplied externally. CHB stage controls cell voltages Vcell, DABs regulate VdcLV, while LV DC/AC stage controls the voltage in the LV port.
3) Grid-feeding in both sides (Fig. 2c). AC voltages in both sides (VacLV and VacHV) are established externally. In this case the LV-side DC/AC converter controls the LV DC link (VdcLV) and the CHB stage controls the cells voltage Vcell. Therefore, DABs connect two ports of constant voltage, behaving as a power source.

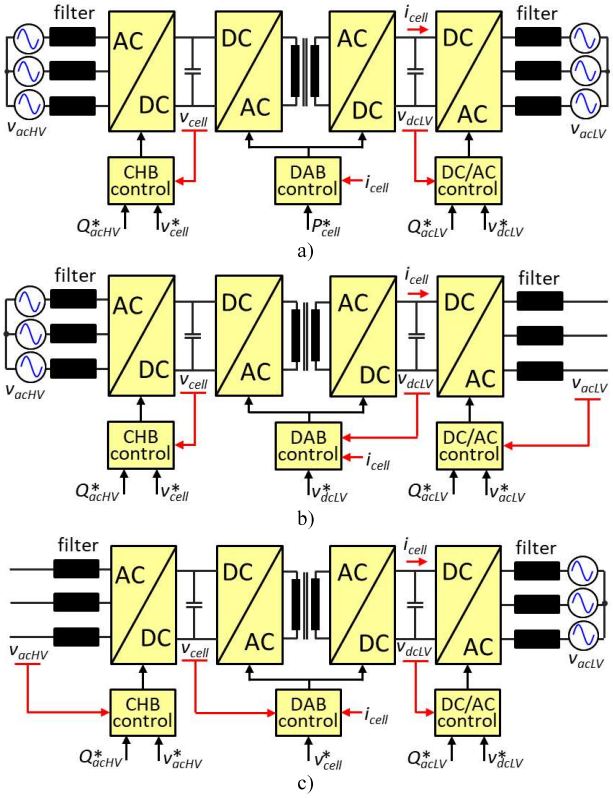

Fig. 2: Modes of operation of the SST. a) Grid feeding in both ports; b) Grid forming at the LV side; c) Grid forming at the HV side. Sinusoidal voltage sources indicate that the corresponding AC port is formed externally. Commands (*) and feedback signals required by the controls are indicated in each case. P and Q stand for active and reactive power respectively. For the sake of simplicity, feedback signals required for other purposes as grid synchronization, inner control loops and protection are not shown.

TABLE I: Main SST Characteristics

	Parameter	*Value*
SST	Rated power	105 kW
	Number of cells	21 (7 per phase)
	HV/LV grid voltage (L-L)	6 kV / 400 V
DAB	Rated power	5 kW
	Switching frequency	30 kHz
	HFT isolation	24 kV
CHB	Rated power	5 kW
	V_{cell}	800 V
	C_{cell}	600 µF(film)
LV DC/AC	Rated power	105 kW
	V_{dcLV}	800 V
	C_{dcLV}	1500 µF (film)
APS_{LV} & APS_{HV}	Input voltage	800 V
	Output voltage	24 V
	Threshold (turn-on)	350 V

II. CELL AND SST START-UP

A methodology to start-up the cells and the SST using APSs fed from the DC links is proposed in this section. The method is valid for all the three modes of operation described in Section II. Fig. 3 shows the cell structure which is seen to consist of two FBs in the HV side and one FB in the LV side. As already mentioned, APSs need a minimum input voltage to turn on. FBs in the HV side will be controllable once APS_{HV} turns on. FBs in the LV and LV-side DC/AC converter will be controllable once APS_{LV} turns on.

A. *Pre-charge circuit*

Pre-charge resistors (R_{PC_cell} and R_{PC_LV} in Fig. 3) are connected in both ports to limit the inrush current flowing through freewheeling diodes (CHB stage or LV-side DC/AC) when the SST is connected to either HV or LV grids through the corresponding switchgear. Pre-charging resistors are bypassed once the DC links stabilize at the rectified voltage values. Pre-charging resistors and bypassing contactors in the LV side can be the same as those used normally in low-voltage DC/AC power converters. Two different options exist for the HV side. Pre-charging resistors and bypassing contactors can be connected at the input of the CHB stage (see Fig. 1). However, this solution requires high voltage resistors and contactors (6 kV in this case), significantly increasing the cost. Alternatively, charging resistors and contactors can be distributed along the cells (left side of Fig. 3). While this implementation obviously requires a larger count of resistors and contactors, they can now be low voltage components, which are significantly cheaper and easier to install. A distributed solution will be used in this work.

Selection of pre-charge resistors is made based on the desired time constant for the resulting RC circuit. A time constant of ≈600 ms has been selected. From the capacitors values shown in Table I, the values for the pre-charge resistors for the HV and LV sides are selected to be 1 kΩ and 450 Ω.

B. *Start-up of three-stage SST strategies*

The proposed procedure partially synchronizes the DC-links charging to suppress the inrush current while controlling the possible SST transients to ensure continuous operation of the APSs. Implementation of the proposed method for the three scenarios described in Section II is discussed in detail following.

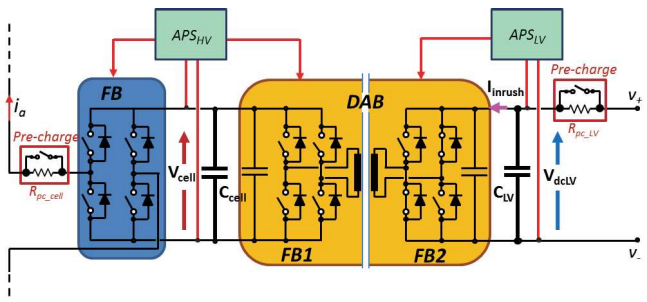

Fig. 3: Cell of the modular SST topology. The LV side DC/AC stage converter is not shown for simplicity.

Grid-forming in the HV side, grid-feeding in the LV side

This scenario assumes that the SST is connected to the LVAC grid and is required to create the MV/HVAC grid. The energization and start-up procedure is schematically shown in Fig. 4, it is seen to consist of seven steps:

1. Grid switchgear enabled: V_{dcLV} increases up to LVAC grid rectified voltage $V_{dcLV} = 650$ V. Transient time constant is determined by pre-charge resistors and C_{LV}.
2. Input voltage to APS_{LV} reaches the threshold voltage and turns on; DAB FB2 and LV side DC/AC converter become operative.
3. DAB FB2 is controlled to charge C_{cell} through FB1 diodes.
4. Input voltage to APS_{HV} reaches the threshold voltage and turns on. DAB FB1 and the CHB FB become operative.
5. V_{cell} and V_{dcLV} match the corresponding grid rectified voltage. Pre-charge resistors are bypassed.
6. V_{dcLV} and V_{cell} are boosted to their target by the LV DC/AC power converter and the DAB FB2 respectively.
7. SST control enabled. DABs controls V_{cell} by controlling the current transferred by the DAB using phase-shift control. CHB stage forms the HVAC grid voltage.

Fig. 5 shows the response of the proposed method obtained by means of simulation. The inrush current and the voltage sag in C_{LV} when the DAB starts charging C_{cell} are readily observed from Fig. 5b and 5c. Inrush current is limited by proper selection of DAB FB2 duty-cycle [22]. One observed inconvenience is the voltage sag in V_{cell} in Fig. 5a when the CHB starts forming the voltage at the HV side (step 7). This corresponds to the inrush current taking place at the same instant. However, it is shown that being able to limit the peak inrush current, both sag magnitudes are not enough to switch off the corresponding APS.

Grid-forming in the LV side, grid-feeding in the HV side

The SST is connected to the MV/HVAC grid and is required to create the LVAC grid voltage. Energization and start-up procedure is schematically shown in Fig. 6. As in the previous case, it consists of seven steps:

1. Grid switchgear enabled: Cell voltage increases up to the corresponding HVAC grid rectified voltage $V_{cell} = 606$ V.

$$V_{cell} = \frac{\sqrt{2} \cdot V_{acHV-line}}{2 \cdot n_{cell}} \quad (1)$$

2. Input voltage to APS_{HV} reaches the threshold voltage and turns on; DAB FB1 and CHB FB become operative.
3. DAB FB1 is controlled to charge C_{LV} through FB2 diodes.
4. Input voltage to APS_{LV} reaches the threshold voltage and turns on. DAB FB2 and LV side converter become operative.
5. V_{cell} and V_{dcLV} match the corresponding grid rectified voltage. Pre-charge resistors are bypassed.
6. V_{cell} and V_{dcLV} are simultaneously boosted to their target by CHB FB and DAB FB1 respectively. Although CHB FB is operative at step (2), its control is not enabled until step (6) to avoid the control working in its critical limits.
7. SST control enabled. DAB controls V_{dcLV}, LV side DC/AC converter forms LVAC grid.

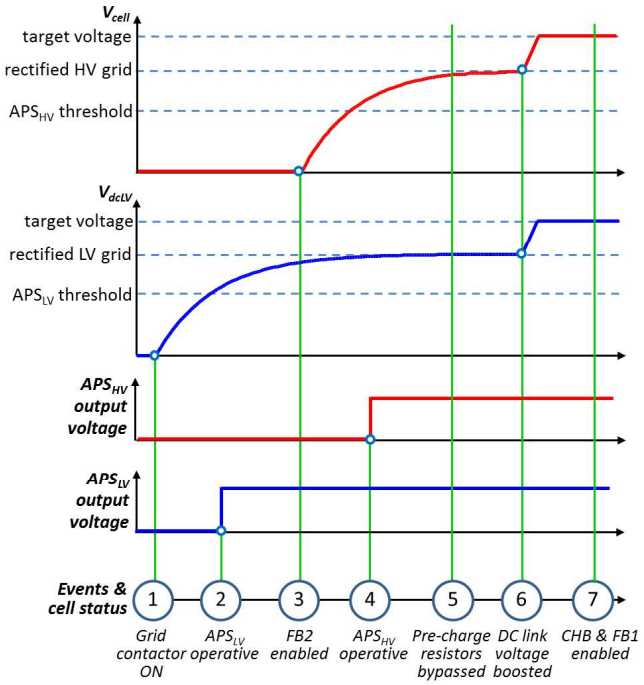

Fig. 4: Proposed start-up procedure when the SST operates in grid forming in the HV side (i.e. energizing from the LV side).

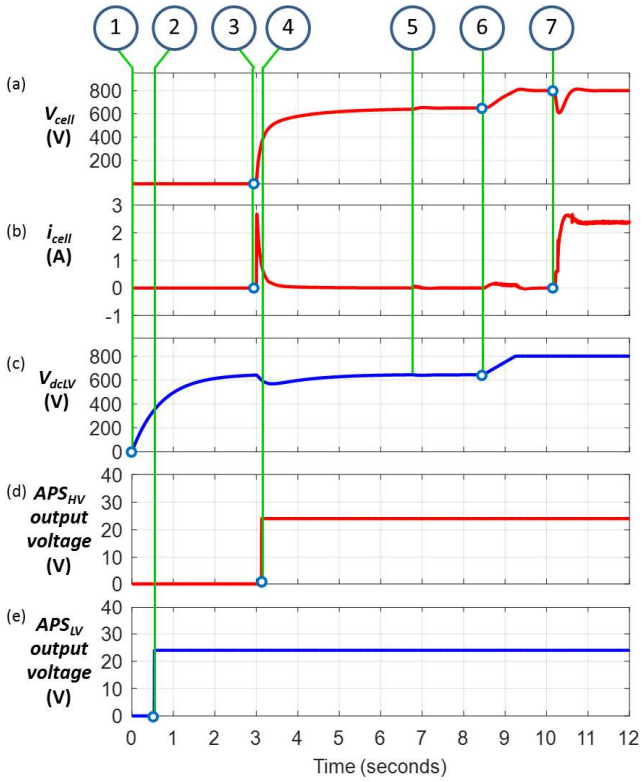

Fig. 5: Simulation results. Proposed start-up procedure for grid-forming in the HV side. a) Cell voltage V_{cell}, b) cell current; c) V_{dcLV}; d) APS_{HV} output voltage, e) APS_{LV} output voltage. Event numbers correspond to those shown in Fig. 4.

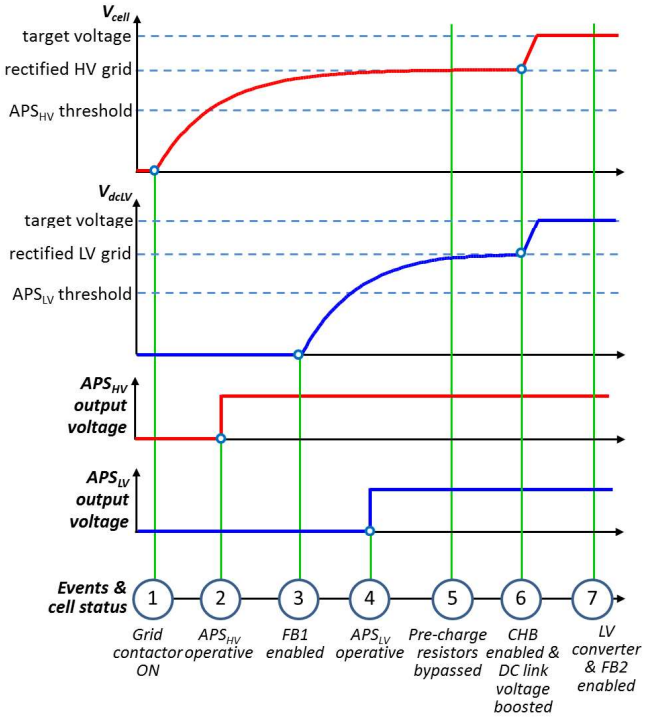

Fig. 6: Proposed start-up procedure when the SST operates in grid-forming in the LV side (i.e. energizing from the HVAC grid).

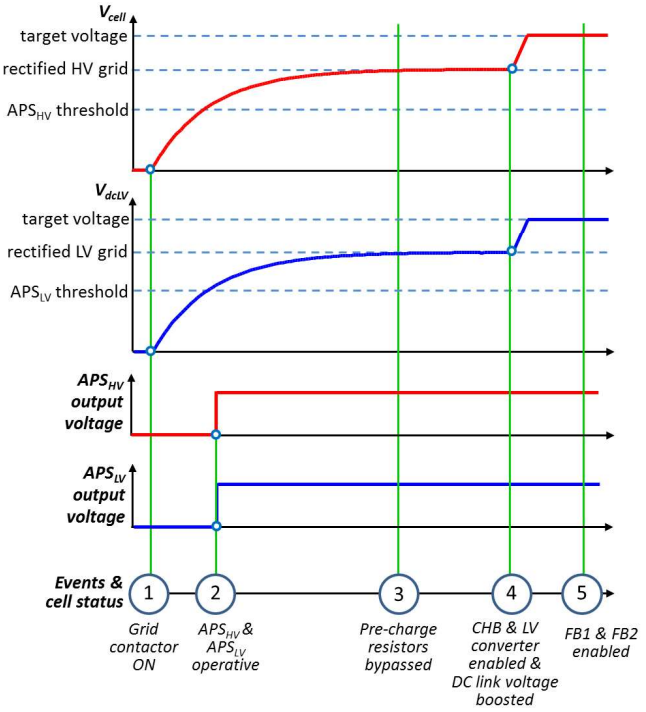

Fig. 7: Proposed start-up procedure when the SST operates in grid-feeding mode. (i.e. Synchronizing rectifier and DC/DC start-up procedure).

LV and HV ports exist, SST operates in a grid-feeding mode

In grid-feeding operation mode, the SST has to transfer power between two existing grids. Energization of the SST is relatively simpler in this case, it is discussed for completeness. The start-up in this case can use the solution of synchronizing the rectifier and DC/DC start-up [16]. The energization and start-up procedure is schematically shown in Fig. 7 and consist of five steps:

1. Grid contactors enabled at both ports: V_{cell} and V_{dcLV} increase synchronously up to the corresponding rectified voltages, V_{cell}=606 V and V_{dcLV} =650 V.
2. Input voltages to APS_{HV} and APS_{LV} reach the threshold voltages and turn on; all the three stages of the SST become operative.
3. Pre-charge resistors are bypassed.
4. V_{cell} and V_{dcLV} are simultaneously boosted to their target value by CHB FBs and LV converter.
5. SST control enabled. DABs control the power transfer between grids using phase shift control.

III. Experimental Verification of Cell Energization and Start-up

The proposed method has been verified experimentally in the cell shown in Fig. 8. The design is the same as the schematically shown in Fig. 4. HFT provides 24 kV isolation between HV and LV sides. Cells are integrated in the SST; its structure is the same as in Fig. 1. Main characteristics of all the elements are listed in Table I. Cell in Fig. 8 is fully operative; SST is currently at a commissioning stage.

The control is carried out in an FPGA-based platform (i.e slave unit in Fig. 8). Fig. 9 shows the start-up process performing grid-forming the HV side (sequence in Fig. 4), which corresponds to the simulation results shown in Fig. 5. In this case the local controller is supplied from APS_{LV}.

Simulated and experimentally measured cell voltage are overlapped in Fig. 10, the agreement being remarkable. Reliability of simulation model is a key for the validation of the whole SST start-up process by simulation discussed in Section V.

IV. Simulation of SST Energization and Start-up

Due to practical limitations, the whole SST start-up cannot be experimentally tested. However, the proposed start-up procedure has been validated in a cell using experimental and simulation results. Thanks to the reliability of the presented simulation model (Fig. 10), a detailed simulation of the full three-phase SST can be used to validate its start-up using the proposed method.

The details related with the full three-phase SST are taken into consideration in the simulation, e.g. the grid filters, the CHB balancing control, the transients in the line voltages and currents, etc. Fig. 11 shows the simulation results in the case of grid-forming in the LV side (see Fig. 6). Inrush currents and voltage sags are under control and consequently turn-off of the APSs are avoided, confirming that the proposed method is valid for the energization of the modular three-stage SST.

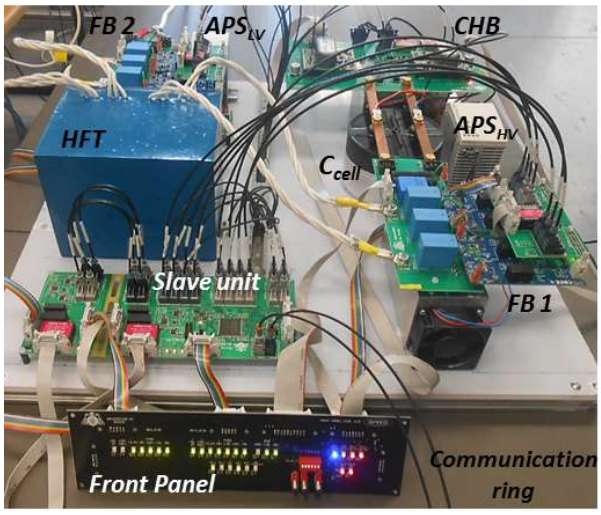

Fig. 8: Cell prototype.

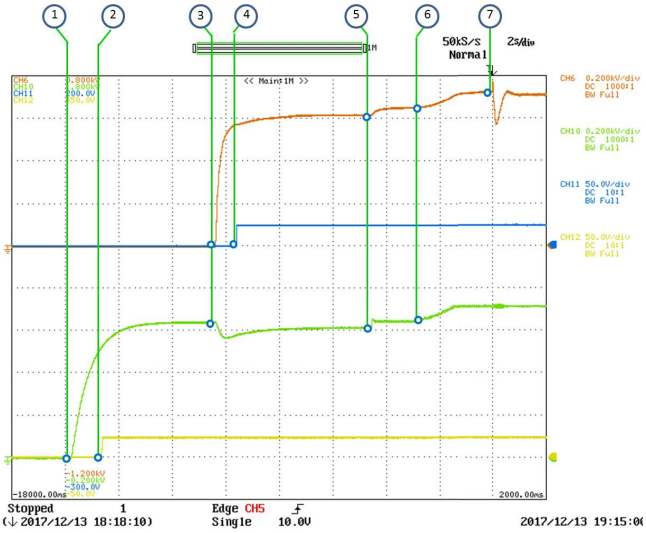

Fig. 9: Experimental results. Grid-forming in the HV side. Top: V_{cell} and APS_{HV} output voltage; Bottom: V_{dcLV} and APS_{LV} output voltage. Event numbers shown on top of the figure correspond to those shown in Fig. 4.

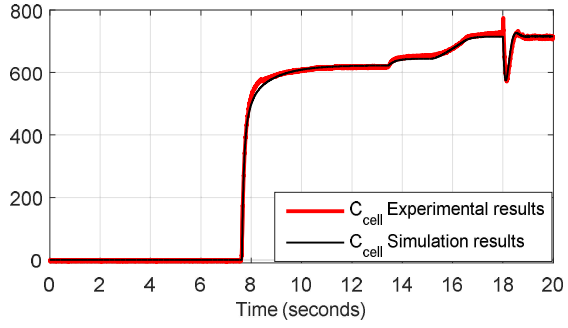

Fig. 10: Simulated and experimentally measured cell voltage during start-up performing grid forming the HV side.

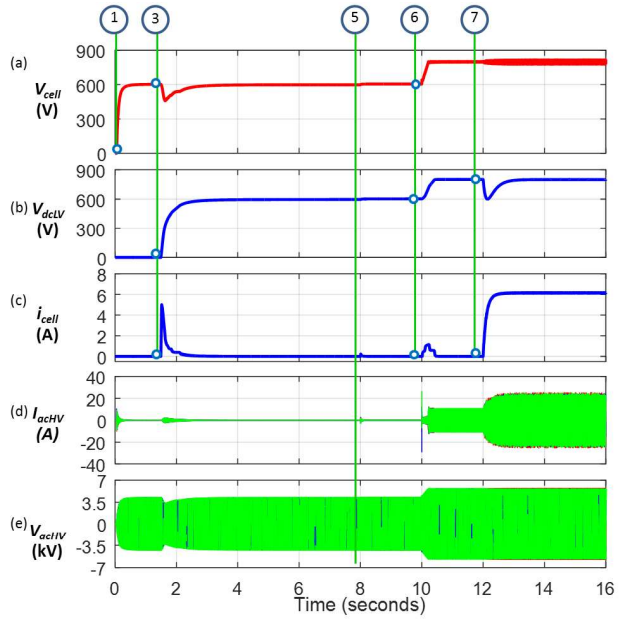

Fig. 11: Proposed SST start-start-up in the case of grid-forming the LV side, a) V_{cell} voltage of the first cell in phase A b) V_{dcLV} voltage, c) Cell current (i_{cell}), d) HVAC grid line currents (i_{acHV}) and e) HVAC grid line voltages (V_{acHV}). Event numbers shown on top of the figure correspond to those shown in Fig. 9.

V. CONCLUSIONS

Energization and start-up process of modular three-stage SSTs based on a cascaded CHB topology have been discussed in this paper. APSs required to feed the auxiliary circuitry can be fed from the cell capacitors. While this enormously simplifies the isolation requirements of the APSs, it implies that the initial stages of SST energization process occur without control. Furthermore, if the SST is intended to operate in a grid-forming mode, energization of its secondary side must be performed from the primary side without any feedback or control. This can result in uncontrolled events (inrush currents, voltage sags in the capacitors voltages, etc.) which could prevent proper energization and start-up of the SST, or even jeopardize the power devices or other elements. A procedure to start-up the SST avoiding such undesirable effects has been proposed. The method is valid for any configuration of the SST (grid-forming/grid-feeding). Simulation results both for the cell and for the SST have been provided to demonstrate the viability of the proposed concepts. Experimental results showing the start-up of a cell have also been provided.

ACKNOWLEDGMENT

This work was supported by the Spanish Government under projects DPI2014-56358-JIN and MINECO-17-DPI2016-75760-R and by the European Commission FP7 Large Project under grant UE-14-SPEED-604057.

REFERENCES

[1] W. McMurray, "Power converter circuits having a high-frequency link," U.S. Patent 3517300, June 23, 1970.

[2] J. W. van der Merwe and H. du T. Mouton, "The solid-state transformer concept: A new era in power distribution," in *AFRICON, 2009*, pp. 1–6.

[3] E. R. Ronan, S. D. Sudhoff, S. F. Glover, and D. L. Galloway, "A power electronic-based distribution transformer," in *IEEE Trans. Power Del.*, vol. 17, no. 2, pp. 537–543, Apr. 2002.

[4] J. Kolar and G. Ortiz, "Solid-state-transformers: Key components of future traction and smart grid systems," presented at the *Int. Power Electronics Conf. (IPEC)*, Hiroshima, Japan, 2014.

[5] M. Steiner and H. Reinold, "Medium frequency topology in railway applications," in *Proc. European Conf. Power Electronics and Applications*, 2007, Aalborg, Denmark, pp. 1–10.

[6] S. Falcones, M. Xiaolin, and R. Ayyanar, "Topology comparison for solid state transformer implementation," in *Proc. IEEE Power and Energy Society General Meeting*, 2010, pp. 1–8.

[7] C. Zhao, D. Dujic, A. Mester, J. K. Steinke, M. Weiss, S. Lewdeni-Schmid, T. Chaudhuri, and P. Stefanutti, Philippe, "Power electronic traction transformer: Medium voltage prototype," *IEEE Trans. Ind. Electron.*, vol. 61, no. 7, pp. 3257–3268, July 2014.

[8] M. Malinowski, K. Gopakumar, J. Rodriguez and M. A. Perez, "A Survey on Cascaded Multilevel Inverters," in *IEEE Transactions on Industrial Electronics*, vol. 57, no. 7, pp. 2197-2206, July 2010.

[9] G. Ortiz, M. G. Leibl, J. E. Huber and J. W. Kolar, "Design and Experimental Testing of a Resonant DC–DC Converter for Solid-State Transformers," in *IEEE Transactions on Power Electronics*, vol. 32, no. 10, pp. 7534-7542, Oct. 2017.

[10] N. B. Y. Gorla, S. Kolluri, P. J. Chauhan and S. K. Panda, "A fault tolerant control approach for a three-stage cascaded multilevel solid state transformer," *2017 IEEE 18th Workshop on Control and Modeling for Power Electronics (COMPEL)*, Stanford, CA, 2017, pp. 1-6.

[11] S. Xu, S. Lukic, A. Q. Huang, S. Bhattacharya, and M. Baran, "Performance evaluation of solid state transformer based microgrid in FREEDM systems," in Proc. *26th Annual IEEE Applied Power Electronics Conf. and Exposition (APEC)*, 2011, pp. 182–188.

[12] T. Zhao, G. Wang, S. Bhattacharya, and A. Q. Huang, "Voltage and power balance control for a cascaded H-bridge converter-based solid state transformer," *IEEE Trans. Power Electron.*, vol. 28, no. 4, pp. 1523–1532, Apr. 2013.

[13] European Union. Advanced power converter for universal and flexible power management in future electricity networks, UNIFLEX, FP6, EC Contract n: 019794 (SES6) European Commission, Directorate J-Energy.

[14] K. Mainali, S. Madhusoodhanan, A. Tripathi, D. Patel and S. Bhattacharya, "Start-up scheme for solid state transformers connected to medium voltage grids," *2015 IEEE Applied Power Electronics Conference and Exposition (APEC)*, Charlotte, NC, 2015, pp. 1014-1021.

[15] X. Liu, L. Liu, H. Li, K. Corzine and T. Guo, "Study on the start-up schemes for the three-stage solid state transformer applications," *2012 IEEE Energy Conversion Congress and Exposition (ECCE)*, Raleigh, NC, 2012, pp. 3528-3532.

[16] X. Liu, H. Li and Z. Wang, "A Start-Up Scheme for a Three-Stage Solid-State Transformer With Minimized Transformer Current Response," in *IEEE Transactions on Power Electronics*, vol. 27, no. 12, pp. 4832-4836, Dec. 2012.

[17] L. B. Kehler, A. M. Kaminski, J. R. Pinheiro, C. Rech, T. B. Marchesan and R. R. Emmel, "Auxiliary power supply for solid state transformers," *2016 IEEE International Conference on Electronics, Circuits and Systems (ICECS)*, Monte Carlo, 2016, pp. 193-196.

[18] D. Cottet *et al.*, "Integration technologies for a medium voltage modular multi-level converter with hot swap capability," *2015 IEEE Energy Conversion Congress and Exposition (ECCE)*, Montreal, QC, 2015, pp. 4502-4509.

[19] A. Rodriguez et al., "Auxiliary power supply based on a modular ISOP flyback configuration with very high input voltage," in *IEEE Energy Conversion Congress and Exposition (ECCE)*, Milwaukee, WI, 2016, pp. 1-7.

[20] F. Briz, M. Lopez, A. Rodriguez and M. Arias, "Modular Power Electronic Transformers: Modular Multilevel Converter versus Cascaded H-Bridge Solutions," IEEE *Industrial Electronics Magazine*, vol. 10, no. 4, pp. 6-19, Dec. 2016.

[21] M. López, F. Briz, M. Saeed, M. Arias and A. Rodríguez, "Comparative analysis of modular multiport power electronic transformer topologies," *2016 IEEE Energy Conversion Congress and Exposition (ECCE)*, Milwaukee, WI, 2016, pp. 1-8.

[22] S. Inoue and H. Akagi, "A Bidirectional DC–DC Converter for an Energy Storage System with Galvanic Isolation," in *IEEE Transactions on Power Electronics*, vol. 22, no. 6, pp. 2299-2306, Nov. 2007.